

Correlating Molecule Count and Release Kinetics with Vesicular Size Using Open Carbon Nanopipettes

Keke Hu, Rui Jia, Amir Hatamie, Kim Long Le Vo, Michael V. Mirkin, and Andrew G. Ewing*



Cite This: *J. Am. Chem. Soc.* 2020, 142, 16910–16914



Read Online

ACCESS |



Metrics & More



Article Recommendations



Supporting Information

ABSTRACT: In this work, open carbon nanopipettes (CNPs) with radius between 50 and 600 nm were used to control translocation of different-sized vesicles through the pipette orifice followed by nanoelectrochemical analysis. Vesicle impact electrochemical cytometry (VIEC) was used to determine the number of catecholamine molecules expelled from single vesicles onto an inner-wall carbon surface, where the duration of transmitter release was quantified and correlated to the vesicle size all in the same nanopip. This in turn allowed us to both size and count molecules for vesicles in a living cell. Here, small and sharp open CNPs were employed to carry out intracellular VIEC with minimal invasion and high sensitivity. Our findings with VIEC reveal that the vesicular content increases with vesicle size. The release kinetics of vesicular transmitters and dense core size have the same relation with the vesicle size, implying that the vesicular dense core size determines the speed of each release event. This direct correlation unravels one of the complexities of exocytosis.

Exocytosis is the key process for cell-to-cell communication in endocrine cells and neurons. It is mediated by neurotransmitter release from nanometer-sized secretory vesicles. These vesicles can be roughly divided into two main types according to their size and different components: small synaptic vesicles (SSVs) and large dense core vesicles (LDCVs). SSVs are smaller types and appear clear in transmission electron microscopy (TEM) images. LDCVs contain two compartments: a fast compartment called the halo with soluble and freely moving transmitters and a slow compartment consisting of a protein core with bound transmitters.^{1–4} LDCVs are present in a number of biological systems. Adrenal chromaffin cells, the widely used model system for exocytosis studies, contain a great number of LDCVs, making up 30% of the total cellular volume.⁵

The amount of catecholamine molecules inside a vesicle is one of the regulators that affect exocytosis.⁶ It is imperative to obtain vesicular content to understand regulation mechanisms of exocytosis. In 2009 Omiatek et al. combined capillary electrophoresis and microfluidics with electrochemical detection to quantify vesicular content.⁷ Later, Dunevall et al. characterized the content of mammalian vesicles by direct absorption and rupture of vesicles on 33 μm diameter disk-shaped carbon electrodes, a technique termed vesicle impact electrochemical cytometry (VIEC).⁸ After that, several studies were carried out aiming to understand the potential mechanisms regarding vesicle opening and rupture on the surface of the electrodes during VIEC.^{9–12}

In addition to vesicular content, quantification of the transmitter concentration in individual vesicles and the correlation between vesicular size and content is important for a comprehensive understanding of the mechanisms of exocytosis. Recently, Zhang et al. reported quantification of vesicular size and catecholamine content at the same time by a combination of resistive pulse measurements with VIEC to

calculate the catecholamine concentrations of single chromaffin vesicles, providing quantitative information about the vesicle maturation process.¹³ Pan et al. showed that translocation of single liposomes and release of loaded dopamine can be monitored simultaneously using open carbon nanopipettes (CNPs).¹⁴

Another aspect that could be influential in exocytotic regulation is the speed or temporal regulation of release events. It has been suggested that release of transmitters bound to proteins filled inside the dense core could be delayed because of their slower diffusion into the extracellular space.^{15,16} Lovrić et al. combined TEM with nanoscale secondary ion mass spectrometry (NanoSIMS) images of a single vesicle and distinguished the distribution of labeled dopamine across the dense core and halo.¹⁷ Correlating the imaged amounts of dopamine in vesicles obtained from NanoSIMS with those from electrochemical methods, they concluded that dopamine loading/unloading between the dense core and halo solution is a kinetically limited process, revealing that both loading of messengers and release into and out of the nanometer protein dense core occur on time scales on the order of hours.

The development of the above methodologies has enriched our knowledge of fundamental mechanisms of exocytosis, yet much remains unknown, especially the correlation between the vesicular structure and release dynamics. CNPs prepared by chemical vapor deposition (CVD) of carbon into prepurged

Received: July 3, 2020

Published: September 16, 2020



quartz nanopipettes have proven to be applicable to electroactive transmitter detection.^{18,19} After modification with Pt black, they were also employed in measurements of reactive oxygen and nitrogen species inside single organelles and vesicles.^{20,21} In this work, we controlled the orifice size of open CNPs in VIEC measurements, and the distribution of $N_{\text{molecules}}$ was correlated with the vesicle size. The general trends of vesicular content and release kinetics with vesicle size were obtained. By comparison of the variations in the release kinetics and dense core size according to vesicle size, a direct connection between the speed of release events and the dense core size was created. Finally, we demonstrate a measurement of combined intracellular VIEC (IVIEC) and vesicle size with an open CNP in a living cell.

Figure 1A shows a schematic of the VIEC measurement with an open CNP. The sizes of single vesicles allowed to diffuse

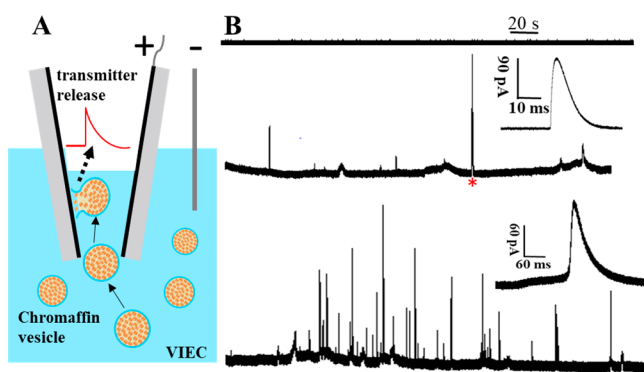


Figure 1. VIEC measurement with different-sized open CNPs. (A) Schematic of VIEC measurement in homogenizing buffer with open CNPs. (B) Representative amperometric traces of 100, 200, and 400 nm radius open CNPs (from top to bottom) at 700 mV vs Ag/AgCl. The insets show amplifications of the spikes labeled with red asterisks.

into the infinite cavity were controlled by adjusting the CNP size (TEM images of CNPs are shown in Figure S1). Oxidation of messenger molecules from single vesicles bursting on the electrode inside the nanotip results in a current transient at the CNP. Representative amperometric traces recording the contents of individual vesicles are presented in Figure 1B. Altogether eight radii of CNPs were used: 50, 100, 200, 250, 300, 400, 500, and 600 nm. Amperometric traces of 50 and 100 nm CNPs gave no spikes, indicating that there were essentially no vesicles below 100 nm radius (Figure 1B), consistent with results from TEM images. Current transients mostly with smaller I_{max} and time duration started to be observed with 200 nm CNPs, coming from rupture of vesicles with sizes between 100 and 200 nm, while with 400 nm CNPs a larger number of bursts were captured. (Additional amperometric traces of CNPs are shown in Figure S2). It should be noted that this approach is different from electrochemical resistive-pulse sensing,¹⁴ as no redox mediator is added in the suspension of vesicles and the vesicle sizes are grouped by the use of different pipette tip sizes. Important information about the release event can be obtained by analyzing the individual spikes. The number of electroactive molecules expelled from individual vesicles can be quantified based on Faraday's law, $N_{\text{molecules}} = N_A Q/nF$, where N_A is Avogadro's number, Q is the charge calculated by integration of the current over time for individual spikes, n is number of electrons transferred during the oxidation reaction ($n = 2$ for

catecholamines), and F is the Faraday constant. The numbers of catecholamine molecules ($N_{\text{molecules}}$) corresponding to spikes of different-sized CNPs were quantified and are presented as normalized frequency histograms in Figure 2.

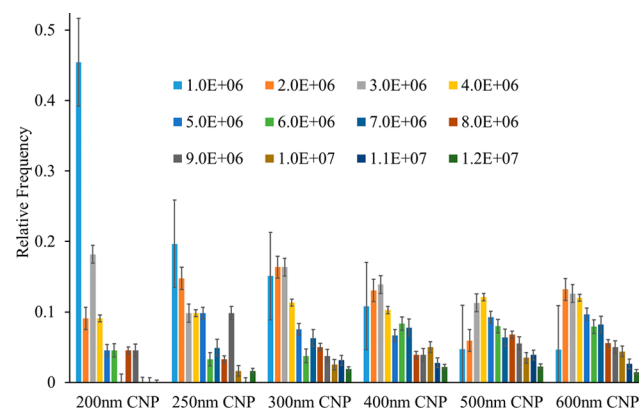


Figure 2. Normalized frequency histograms of $N_{\text{molecules}}$ obtained from different-sized open CNPs (200, 250, 300, 400, 500, and 600 nm radius). (Bin size, 1×10^6 molecules; collected from four isolations of adrenal chromaffin vesicles; 98 open CNPs were used).

Markedly different ratios of $N_{\text{molecules}}$ (bin size of 1×10^6 molecules) across different-sized CNPs are shown in Figure 2. For vesicles smaller than 200 nm, vesicles containing 1×10^6 transmitters make up 45% of the total number of vesicles, and this ratio keeps decreasing as the vesicle size increases up to 500 nm. Also, the largest $N_{\text{molecules}}$ for vesicles below 200 nm is within 9×10^6 , which is quite different from their counterparts. The ratio of vesicles with larger contents of transmitters generally increases with vesicle size. For vesicles below 250 nm, vesicles with lowest number of transmitters (1×10^6) account for the biggest percentage, and that ratio decreases with vesicular content. For larger vesicles, the frequency of vesicles first goes up and then goes down, with peaks mostly appearing at contents of 2×10^6 and 3×10^6 molecules. It should be noted that there is a slight change in distribution from 500 to 600 nm CNPs, implying that the sizes of a small number of vesicles are above 500 nm. This was further confirmed by comparison of the averages of vesicular content and release kinetics between 500 and 600 nm CNPs in Figure 3A and the results of TEM imaging in Figure 3B.

As shown in Figure 3A, from 200 to 500 nm CNPs, the average vesicular content increases with vesicle size, which makes sense considering the distribution of $N_{\text{molecules}}$ over size in Figure 2. Apart from $N_{\text{molecules}}$, the duration of messenger release ($t_{1/2}$), the time needed for the fusion pore to open (t_{rise}), and the time for oxidation of vesicular content or for the pore to close again (t_{fall}) can also be quantified by analyzing individual current transients.²² The release kinetics versus vesicle size is presented in Figure 3A with similar numbers for 500 and 600 nm CNPs. In contrast to the trend line of vesicular content, the duration of chemical messenger release first increases with vesicle size, peaks for 400 nm CNPs, and beyond that decreases substantially. The same trends of t_{rise} and t_{fall} are presented in Figure S3. As discussed before, aggregated protein in the vesicular dense core can slow the release of chemical messengers.^{15,16} It is possible that changes in the release kinetics are related to the dense core size. By measurement of the dense core size from TEM images of chromaffin cells (Figure S4), the dense core size was obtained

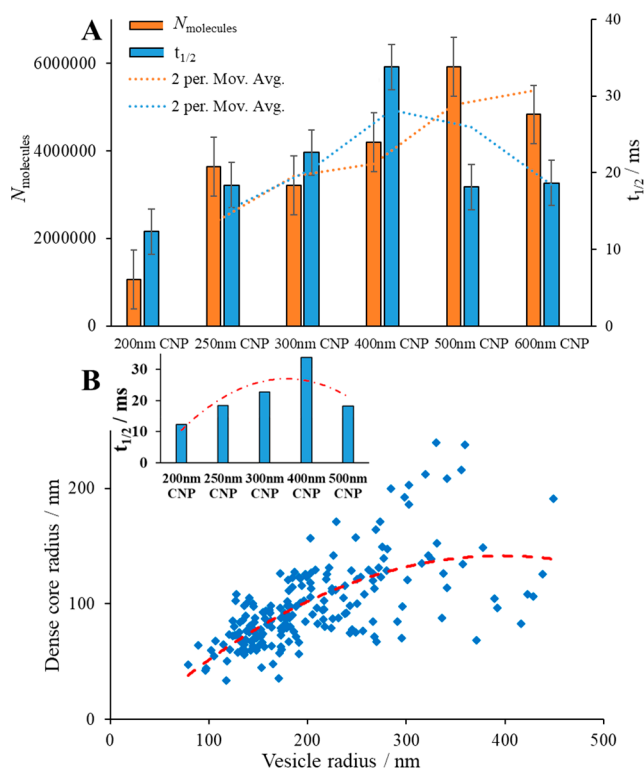


Figure 3. Correlations of vesicular content and release kinetics with vesicle size. (A) Histograms of average $N_{\text{molecules}}$ and $t_{1/2}$ derived from different-sized open CNPs with trend lines (two-period moving average). (B) TEM data on vesicle dimensions with a trend line (second-order polynomial). The inset shows a histogram of $t_{1/2}$ for 200 to 500 nm open CNPs with a trend line (second-order polynomial). $N_{\text{molecules}}$ and $t_{1/2}$ are medians obtained from each size of open CNPs; specific numbers are listed in Table S1. The dense core radius and vesicle radius were measured from TEM images of chromaffin cells (Figure S4).

as a function of vesicle size. The trend line in Figure 3B shows that the dense core size increases with vesicle size up to ~ 380 nm, whereas after that dense core size drops significantly and almost all of the points are below the trend line. Although the data are somewhat scattered at the larger sizes, there is a corresponding trend with the change in release kinetics (see the Figure 3B inset). We conclude that the kinetics of chemical messenger release is limited by the dense core size.

In addition to VIEC, open CNPs were used to carry out IVIEC of vesicles in living cells. Figure 4 presents an

amperometric trace from an IVIEC measurement inside an $18 \mu\text{m}$ diameter chromaffin cell with a 400 nm radius CNP. The red arrow indicates the moment when the CNP was pushed through the cell membrane. After a slight vibration, the CNP was inserted with a reasonable background current at 700 mV . After IVIEC measurements, both $18 \mu\text{m}$ and $13 \mu\text{m}$ diameter chromaffin cells maintained no observable morphological changes (Figures S5 and S6), suggesting that the cells and cell functions were not dramatically altered. For intracellular use, it is crucial for biological cells to maintain their integrity and viability. Although the tip size of CNPs is relatively large compared with the commonly used nanotip carbon fiber microelectrodes in IVIEC measurements,^{23,24} here only a small portion of the tip end pierced into the cytoplasm, allowing vesicles together with cytosol to be driven into pipettes by capillary action or diffusion. As can be seen from the amperometric trace in Figure 4, an increased frequency of rupture events was observed about 25 s after the CNP was inserted. For intracellular electrochemical analysis with nanoelectrodes, trade-offs between scale and sensitivity have been the main issue that needs to be addressed. Despite the small tip size, the hollow structure of open CNPs provides a sufficiently large electrochemical area for oxidation of vesicular transmitters, and this is also critical for in vivo measurements in small organisms. In the future this will allow us to study the correlations of vesicular content and release dynamics with vesicular structure in the intracellular environment and the effect of drug treatment.

In conclusion, we have presented a combination of VIEC with open CNPs for characterization of chemical messengers in single vesicles entering and impacting the electrode in the CNP. With this new method, correlations of the vesicle content and release kinetics with vesicle size can be obtained. Our results demonstrate that the speed of release events depends on the vesicular dense core size. A direct correlation between the vesicular structure and release dynamics was established, and this will offer new insights into regulation of exocytosis, including an unprecedented ability to study the effect of dense core matrix dissociation on the release kinetics. Besides application in VIEC, open CNPs with smaller physical size and larger electroactive surface area are promising for in situ intracellular tests and have potential for in vivo measurements inside small organisms such as *Drosophila*, zebrafish, etc.

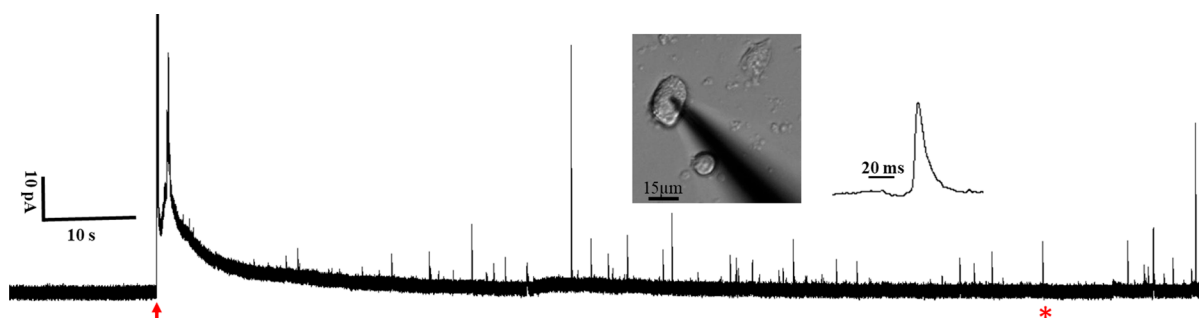


Figure 4. Representative amperometric trace from an IVIEC measurement with a 400 nm radius open CNP at 700 mV vs Ag/AgCl . The inset shows an image of a CNP being inserted into an $18 \mu\text{m}$ diameter chromaffin cell during an IVIEC measurement and an amplification of the spike labeled with the red asterisk. The red arrow indicates the moment when the CNP was pushed through the cell membrane.

■ ASSOCIATED CONTENT

Supporting Information

The Supporting Information is available free of charge at <https://pubs.acs.org/doi/10.1021/jacs.0c07169>.

Experimental details, TEM images of CNPs, additional amperometric traces of CNPs, medians of $N_{\text{molecules}}$ and $t_{1/2}$ with different-sized CNPs, histograms of t_{rise} and t_{fall} and TEM images of chromaffin cells (PDF)

■ AUTHOR INFORMATION

Corresponding Author

Andrew G. Ewing – Department of Chemistry and Molecular Biology, University of Gothenburg, 41296 Gothenburg, Sweden; orcid.org/0000-0002-2084-0133; Email: andrew@chem.gu.se

Authors

Keke Hu – Department of Chemistry and Molecular Biology, University of Gothenburg, 41296 Gothenburg, Sweden

Rui Jia – Department of Chemistry and Biochemistry, Queens College-CUNY, Flushing, New York 11367, United States; The Graduate Center of the City University of New York, New York, New York 10016, United States; orcid.org/0000-0002-6094-982X

Amir Hatamie – Department of Chemistry and Molecular Biology, University of Gothenburg, 41296 Gothenburg, Sweden; orcid.org/0000-0002-7085-893X

Kim Long Le Vo – Department of Chemistry and Molecular Biology, University of Gothenburg, 41296 Gothenburg, Sweden

Michael V. Mirkin – Department of Chemistry and Biochemistry, Queens College-CUNY, Flushing, New York 11367, United States; The Graduate Center of the City University of New York, New York, New York 10016, United States

Complete contact information is available at: <https://pubs.acs.org/doi/10.1021/jacs.0c07169>

Notes

The authors declare no competing financial interest.

■ ACKNOWLEDGMENTS

We acknowledge funding from the European Research Council (Advanced Grant), the Knut and Alice Wallenberg Foundation, the Swedish Research Council (VR), and the U.S. National Institutes of Health. A.H. specifically acknowledges support from Sweden's Innovation Agency (Vinnova) and the Swedish Strategy Group for EU Coordination. M.V.M. acknowledges the support by the U.S. National Science Foundation (CHE-1763337).

■ REFERENCES

- (1) Huttner, W. B.; Gerdes, H. H.; Rosa, P. The granin-(chromogranin/secretogranin) family. *Trends Biochem. Sci.* **1991**, *16*, 27–30.
- (2) Wiedenmann, B.; Huttner, W. B. Synaptophysin and chromogranins/secretogranins widespread constituents of distinct types of neuroendocrine vesicles and new tools in tumor diagnosis. *Virchows Arch. B* **1989**, *58*, 95–121.
- (3) Oleinick, A.; Hu, R.; Ren, B.; Tian, Z.-Q.; Svir, I.; Amatore, C. Theoretical Model of Neurotransmitter Release during In Vivo Vesicular Exocytosis Based on a Grainy Biphasic Nano-Structuration of Chromogranins within Dense Core Matrixes. *J. Electrochem. Soc.* **2016**, *163*, H3014–H3024.

(4) Yao, J.; Erickson, J. D.; Hersh, L. B. Protein Kinase A Affects Trafficking of the Vesicular Monoamine Transporters in PC12 Cells. *Traffic* **2004**, *5*, 1006–1016.

(5) Plattner, H.; Artalejo, A. R.; Neher, E. Ultrastructural Organization of Bovine Chromaffin Cell Cortex—Analysis by Cryofixation and Morphometry of Aspects Pertinent to Exocytosis. *J. Cell Biol.* **1997**, *139*, 1709–1717.

(6) Pothos, E.; Desmond, M.; Sulzer, D. 1-3,4-Dihydroxyphenylalanine Increases the Quantal Size of Exocytotic Dopamine Release In Vitro. *J. Neurochem.* **1996**, *66*, 629–636.

(7) Omiatek, D. M.; Santillo, M. F.; Heien, M. L.; Ewing, A. G. Hybrid Capillary-Microfluidic Device for the Separation, Lysis, and Electrochemical Detection of Vesicles. *Anal. Chem.* **2009**, *81*, 2294–2302.

(8) Dunevall, J.; Fathali, H.; Najafinobar, N.; Lovric, J.; Wigström, J.; Cans, A.-S.; Ewing, A. G. Characterizing the Catecholamine Content of Single Mammalian Vesicles by Collision-Adsorption Events at an Electrode. *J. Am. Chem. Soc.* **2015**, *137*, 4344–4346.

(9) Lovrić, J.; Najafinobar, N.; Dunevall, J.; Majdi, S.; Svir, I.; Oleinick, A.; Amatore, C.; Ewing, A. G. On the mechanism of electrochemical vesicle cytometry: chromaffin cell vesicles and liposomes. *Faraday Discuss.* **2016**, *193*, 65–79.

(10) Li, X.; Dunevall, J.; Ren, L.; Ewing, A. G. Mechanistic Aspects of Vesicle Opening during Analysis with Vesicle Impact Electrochemical Cytometry. *Anal. Chem.* **2017**, *89*, 9416–9423.

(11) Li, X.; Ren, L.; Dunevall, J.; Ye, D.; White, H. S.; Edwards, M. A.; Ewing, A. G. Nanopore Opening at Flat and Nanotip Conical Electrodes during Vesicle Impact Electrochemical Cytometry. *ACS Nano* **2018**, *12*, 3010–3019.

(12) Najafinobar, N.; Lovrić, J.; Majdi, S.; Dunevall, J.; Cans, A. S.; Ewing, A. Excited Fluorophores Enhance the Opening of Vesicles at Electrode Surfaces in Vesicle Electrochemical Cytometry. *Angew. Chem., Int. Ed.* **2016**, *55*, 15081–15085.

(13) Zhang, X.-W.; Hatamie, A.; Ewing, A. G. Simultaneous Quantification of Vesicle Size and Catecholamine Content by Resistive Pulses in Nanopores and Vesicle Impact Electrochemical Cytometry. *J. Am. Chem. Soc.* **2020**, *142*, 4093–4097.

(14) Pan, R.; Hu, K.; Jiang, D.; Samuni, U.; Mirkin, M. V. Electrochemical Resistive-Pulse Sensing. *J. Am. Chem. Soc.* **2019**, *141*, 19555–19559.

(15) Montesinos, M. S.; Machado, J. D.; Camacho, M.; Diaz, J.; Morales, Y. G.; Alvarez de la Rosa, D.; Carmona, E.; Castañeyra, A.; Viveros, O. H.; O'Connor, D. T.; Mahata, S. K.; Borges, R. The Crucial Role of Chromogranins in Storage and Exocytosis Revealed Using Chromaffin Cells from Chromogranin A Null Mouse. *J. Neurosci.* **2008**, *28*, 3350–3358.

(16) Helle, K. B.; Reed, R. K.; Pihl, K. E.; Serck-Hanssen, G. Osmotic properties of the chromogranins and relation to osmotic pressure in catecholamine storage granules. *Acta Physiol. Scand.* **1985**, *123*, 21–33.

(17) Lovrić, J.; Dunevall, J.; Larsson, A.; Ren, L.; Andersson, S.; Meibom, A.; Malmberg, P.; Kurczyk, M. E.; Ewing, A. G. Nano Secondary Ion Mass Spectrometry Imaging of Dopamine Distribution Across Nanometer Vesicles. *ACS Nano* **2017**, *11*, 3446–3455.

(18) Hu, K.; Wang, D.; Zhou, M.; Bae, J. H.; Yu, Y.; Xin, H.; Mirkin, M. V. Ultrasensitive Detection of Dopamine with Carbon Nanopipets. *Anal. Chem.* **2019**, *91*, 12935–12941.

(19) Yang, C.; Hu, K.; Wang, D.; Zubi, Y.; Lee, S. T.; Puthongkham, P.; Mirkin, M. V.; Venton, B. J. Cavity Carbon-Nanopipette Electrodes for Dopamine Detection. *Anal. Chem.* **2019**, *91*, 4618–4624.

(20) Hu, K.; Li, Y.; Rotenberg, S. A.; Amatore, C.; Mirkin, M. V. Electrochemical Measurements of Reactive Oxygen and Nitrogen Species inside Single Phagolysosomes of Living Macrophages. *J. Am. Chem. Soc.* **2019**, *141*, 4564–4568.

(21) Pan, R.; Hu, K.; Jia, R.; Rotenberg, S. A.; Jiang, D.; Mirkin, M. V. Resistive-Pulse Sensing Inside Single Living Cells. *J. Am. Chem. Soc.* **2020**, *142*, 5778–5784.

(22) Mosharov, E. V.; Sulzer, D. Analysis of exocytotic events recorded by amperometry. *Nat. Methods* **2005**, *2*, 651–658.

(23) Li, X.; Majdi, S.; Dunevall, J.; Fathali, H.; Ewing, A. G. Quantitative Measurement of Transmitters in Individual Vesicles in the Cytoplasm of Single Cells with Nanotip Electrodes. *Angew. Chem., Int. Ed.* **2015**, *54*, 11978–11982.

(24) Yue, Q.; Li, X.; Wu, F.; Ji, W.; Zhang, Y.; Yu, P.; Zhang, M.; Ma, W.; Wang, M.; Mao, L. Unveiling the Role of DJ-1 Protein in Vesicular Storage and Release of Catecholamine with Nano/Micro-Tip Electrodes. *Angew. Chem., Int. Ed.* **2020**, *59*, 11061–11065.